Dynamic Measurement of the HMX β-δ Phase Transition by Second Harmonic Generation

B. F. Henson, B. W Asay, R. K. Sander, S. F. Son, J. M. Robinson, and P. M. Dickson
Los Alamos National Laboratory, Los Alamos, New Mexico 87545

(Received 2 June 1998; revised manuscript received 15 October 1998)

We demonstrate the use of optical second harmonic generation (SHG) to identify the β-δ phase transition in polycrystalline HMX. This phase transition has been implicated in the thermal decomposition of HMX for over 30 years. We measure an order of magnitude difference in SHG cross section from the β and δ phases and use this intensity difference to observe the phase transition during CO_2 laser irradiation. This is the first known *in situ* measurement of a phase transition in such an energetic material during a dynamic experiment, and the first example of SHG from this class of organic nitramine molecular crystals. [S0031-9007(98)08215-5]

PACS numbers: 42.65.Ky, 42.70.Jk

Research into the dynamic behavior of energetic materials is a major area of physics. This effort is complicated, however, by the range of structural phases exhibited by many crystalline materials. Development of improved techniques for measuring phase transformations *in situ* is thus of great interest. HMX (octahydro-1,3,5,7-tetranitro-1,3,5,7-tetrazocine) is one such material which exhibits a wide variety of behaviors when subjected to various thermal fields. Temperatures just above 450 K induce explosion after an induction time from 10^5 to 10^1 s [1]. Infrared laser irradiation generates surface temperatures from 500–700 K and ignition at 10^{-3} to 10^1 s [2]. Shear or frictional heating of pressed solids to 700–900 K results in ignition in 10^{-4} s [3]. Planar shocks from 10 to 30 GPa result in detonation over times of 10^{-7} to 10^{-6} s [4]. Despite considerable progress in understanding the chemistry governing these processes, which span twelve decades in time, no comprehensive model of decomposition linking the separate regimes currently exists.

It has been recognized for 30 years [5] that the crystalline phases of HMX may play a role in the decomposition chemistry. Of the four phases of HMX identified [5], two have been of traditional concern, β-HMX, a low temperature form, and δ-HMX, a high temperature form which is the only phase observed upon low pressure heating of all four polymorphs [6]. Differences in burn rate and drop height sensitivity have been shown between the β and δ phases [7], with δ-HMX the more hazardous material. Kinetic measurements of the β-δ transition by Brill *et al.* [6] showed that the first order activation energy and frequency factor resemble those attributed to chemical decomposition, supporting previous speculation by the authors that the initial decomposition step in HMX is coupled to, or preceded by, the formation of δ-HMX [8].

However, no *in situ* measurements of the rate of transformation have been reported for ignition experiments. Identification of the phase and transition rate has relied on traditional calorimetry [4], Fourier transform infrared (FTIR), and Raman techniques [9] addressing times and temperatures of 10^2–10^5 s and 450 to 500 K. The role of the β-δ transition during ignition is therefore completely uncertain, and the validity of extrapolating measured transition rates to ignition times of less than a second has not been established. Currently, the kinetics of the β-δ transition are not incorporated into any of the decomposition mechanisms of HMX, although some combustion models include a parametrization of physical properties which includes the δ phase [10].

We used the nonlinear optical technique, second harmonic generation (SHG), as a fast *in situ* probe of the β-δ transition in HMX [11,12]. We first demonstrate the technique by monitoring the transition during slow heating. The transition temperatures and times are consistent with kinetics reported in the literature [6]. We also report the first observation of the β-δ phase transition during a dynamic ignition experiment. We observe the transition to δ-HMX at the surface of a pressed, polycrystalline sample during laser irradiation at $\lambda \sim 10.6\ \mu\text{m}$ $(20\ \text{W/cm}^2\,\text{s})$ prior to ignition. The transition time and surface temperature are again consistent with low temperature measurements, validating the extrapolation of calculated transition rates to times of 10^{-2} s.

In the present paper, SHG is observed both in transmission through a thin layer of powdered crystal and in reflection from the surface of a pressed polycrystalline pellet. Experiments were first conducted to measure the relative SHG cross sections from both phases of HMX and to observe the phase transition during slow heating. Powdered crystalline samples of a KH_2PO_4 (KDP) standard, and β- or δ-HMX (1–500 μm diameter) were mounted as thin layers of powder ($\sim$500 μm thick) between sapphire windows [13]. This cell was enclosed in an oven and placed in the optical path of a 10 Hz Nd:YAG laser delivering 10 ns pulses at 1064 nm $(10\text{–}100\ \text{MW/cm}^2)$. Diffuse, forward scattered SHG was filtered of 1064 nm fundamental light, focused into a monochromater and detected with a phototube. The scattered intensity followed the square of the input intensity, with no strong dependence on input or detection polarization. The spectrum of SHG from the δ-HMX and KDP was centered at 532 nm and was consistent with the elastic conversion of the 1064 nm input pulse to 532 nm. Illumination of KDP samples

0031-9007/99/82(6)/1213(4)$15.00

with an intensity of 24 MW/cm^2 led to the generation of 532 nm, consistent with the large KDP cross section [11]. Remarkably, the SHG from δ-HMX was within 20% of the intensity measured for KDP. The SHG from β-HMX, by contrast, was lower by a factor of 50 from the δ form. This is consistent with the crystallographic symmetry of the two polymorphs, with β-HMX being a centrosymmetric, monoclinic structure of $P2_1/c$ space group [14] and δ-HMX a noncentrosymmetric, hexagonal structure of space group $P6_122$ [5]. Second harmonic generation in the β polymorph should thus be strongly suppressed relative to the δ phase due to symmetry considerations [11], as we observe. Additionally, the two polymorphs differ in several other respects, with a 7% volume expansion on transformation from β to δ and a change in unit cell participation from two molecules in β to six in δ-HMX. Also, the very polar nitro groups are nearly trans in the β form, and cis in the δ, leading to a significant change in dipole moment and reduction of the molecular point group symmetry upon transition. For applications to thermal decomposition in energetic materials, this difference in cross section for β- and δ-HMX provides excellent contrast for use as an *in situ* probe of the phase transition in dynamic experiments. We stress that this is a nonresonant application of SHG, and, as such provides no spectroscopic identification of any specific HMX polymorph. The demonstrated contrast in cross section for the β- and δ-HMX does, however, allow the use of the SHG intensity to measure the rate of transformation between these polymorphs under conditions where the initial and product phases of HMX have been identified, as is the case for the two experiments described here.

The results of three slow heating experiments with this configuration are shown in Fig. 1. The samples were initially β-HMX. The data are plotted as the SHG intensity (symbols), normalized to the maximum signal, on the left axis, and the temperature (dashed lines), on the right, both as a function of time. The transition to δ-HMX is apparent as a rapid increase in the SHG, occurring at temperatures of approximately 170 C. If one considers the normalized SHG intensity, varying from 0 to 1, as proportional to the δ-HMX mole fraction, these data may be modeled using a kinetic rate law first order in both β and δ, $dc/dt = k\,(\beta_0 - c)(\delta_0 + c)$, where c is the concentration of δ formed, β_0 and δ_0 are the initial concentrations of β- and δ-HMX, respectively, t is the time, and k is an Arrhenius rate expression, $k = A\exp(-Ea/RT)$ [15]. The partially integrated rate law, normalized to β_0, is

$$x(T,t) = \frac{f\exp[\beta_0 \int k(T,t)dt]}{f\exp[\beta_0 \int k(T,t)dt] + 1}, \qquad (1)$$

where x is the fraction of β-HMX converted to δ, and f is the initial ratio of δ to β, δ_0/β_0. The normalized SHG intensity may then be expressed as a function of the δ-HMX fraction and a constant ε which is the ratio of SHG intensity from pure β- and δ-HMX, $I_{2\omega}/I_{2\omega}^{\max} = [\varepsilon(I - x) + x]^2$. The solid lines in Fig. 1 for each data set were calculated with these formulas, utilizing Ea, A, and f as fitting parameters. The optimized parameters were $Ea = 201.6(2.0)$ kJ/mole, $\log(A) = 21.9(0.8)$, A in cm^3/g s, and $\log(f) = -2.6(1.0)$, with the standard deviation at 95% confidence in parentheses. Brill *et al.* [6,8] observed approximate first order behavior for the transition at low levels of conversion and determined the Arrhenius parameters to be $Ea = 204(14)$ kJ/mole and $\log(A) = 19.9(1.0)$1/s, with uncertainty in parentheses. Observation of complete conversion leads to the use of a second order rate law in these experiments. These results are, in fact, consistent with those of Brill *et al.* and serve to quantify the observed SHG as a kinetic probe, yielding Arrhenius parameters consistent with those observed previously, and the assignment of a second order rate law to the process [16]. In addition, although kinetic measurements have been performed for all four HMX polymorphs [6,8], δ-HMX was the only product observed during heating at low pressure. We rely on these and subsequent observations [7] to assign the transition observed in this work to the HMX β-δ transition.

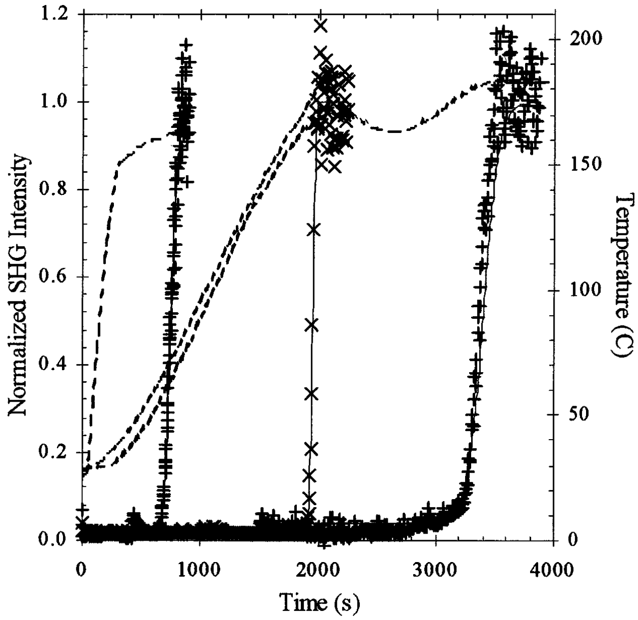

FIG. 1. Data from slow heating of β-HMX. The crosses are the normalized SHG intensity and the dashed lines are the temperature profiles, both as a function of time. The temperature profile of each experiment terminates at roughly the time of transition to δ-HMX, signified by the increase in signal. The solid lines through the data are calculated from Eq. (1).

The configuration used for the laser ignition experiments is shown as an inset of Fig. 2. A pressed pellet of HMX is illuminated by the continuous output of a $\lambda \sim 10.6$ μm CO$_2$ laser. Interference effects from beam integration result in a crosshatched pattern of slight surface temperature variability. Again, 10 Hz Nd:YAG laser

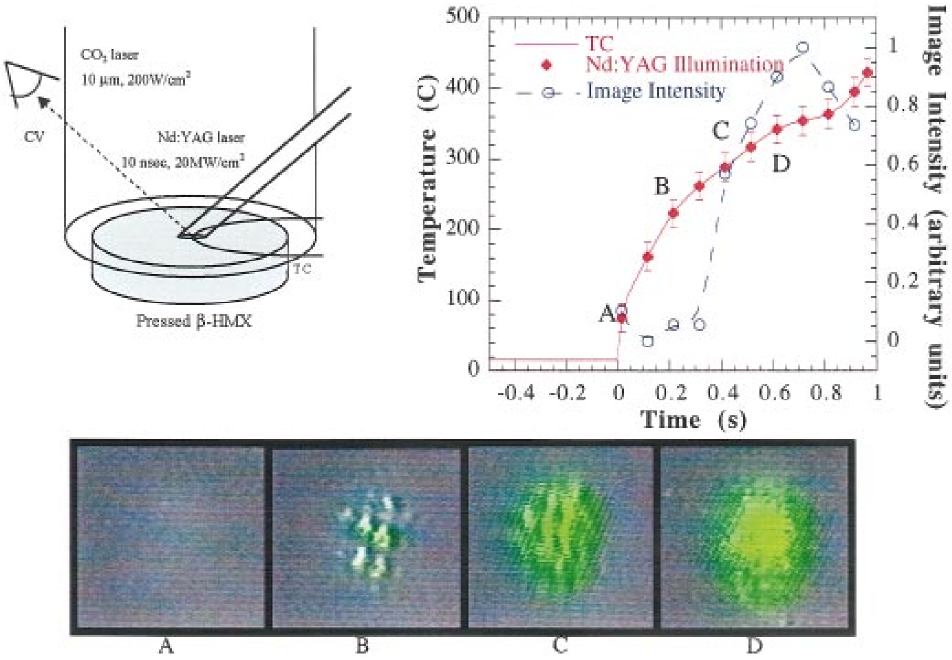

FIG. 2(color). Composite figure showing a schematic of the pressed pellet ignition experiments, including the second harmonic laser, detection, and CO_2 laser illumination axis, the time series data of temperature rise, and imaging of SH and selected images of the pellet surface showing the evolution of the SHG intensity. The plot displays the temperature recorded by a thermocouple as a function of time. The letters indicate the time and temperature at which the images were recorded. TC indicates thermocouple and CV indicates color video camera.

illumination, identical to the previous experiment, was directed onto the surface at an angle of approximately 30° from normal, and a color video camera was used to image the SHG at the surface along the specular reflection axis of the 1064 nm illumination. A 13 μm diameter thermocouple (type K), centered on the 1064 nm illumination spot on the surface, was used to record the temperature during heating. The experiment consisted of beginning CO_2 illumination at t_0 and monitoring the temperature rise until ignition in the gas phase approximately 1 s later. During heating, the SHG emission from the surface was imaged at the video rate of 60 Hz. The temperature, average image intensity as a function of time, and selected images of the SHG appearance are also shown in Fig. 2. The plot displays the temperature recorded by a thermocouple as a function of time. The letters indicate the time and temperature at which the images were recorded. The images are from the video record of the 1064 nm illumination spot. Second harmonic generation first appears at approximately 250 ms, with an uncertainty from the framing rate of 30 ms, and clearly reflects the crosshatched heating pattern on the surface. We take the appearance of SHG to indicate the HMX β to δ phase transition at the surface, and from the average intensity of the video image we determine a transition time of 366(100) ms at a homogeneous surface temperature of 277(30) C. An Arrhenius plot of observed HMX β-δ kinetics is shown in Fig. 3. The solid bar is an average of the data of Brill *et al.* [6]. The dashed lines reflect the uncertainties in rate at higher temperatures which result from extrapolation of these data with the reported uncertainties. The data point which results from this work is plotted as the inverse of the time to transition as a function of inverse temperature and is clearly consistent with the low temperature measurements. This observation constitutes the first experimental verification of the extrapolation of these kinetics to combustion regimes, as first discussed fifteen years ago [17]. More generally, observation of the transition over such a wide range of temperature and time requires serious reconsideration of this transformation as the first elementary step in HMX decomposition, as was first suggested by Brill *et al.* [6,8].

This measurement also represents the first measurement of crystalline phase during a dynamic ignition experiment. Numerous long-standing problems are now amenable to investigation with this probe. For instance, the ignition of heterogeneous explosives subject to strong shock has long been believed to proceed via the mechanical formation of “hot spots” during compression [18]. With a reliable understanding of the transformation kinetics of the various HMX polymorphs, the spatially resolved observation of these phase transitions via SHG may provide a new avenue for the first experimental observation of these localized regions of heating.

Finally, we have begun to address the generality of this technique by application to other energetic materials. To date, we have demonstrated both considerable absolute SHG efficiency and strong temperature dependence for

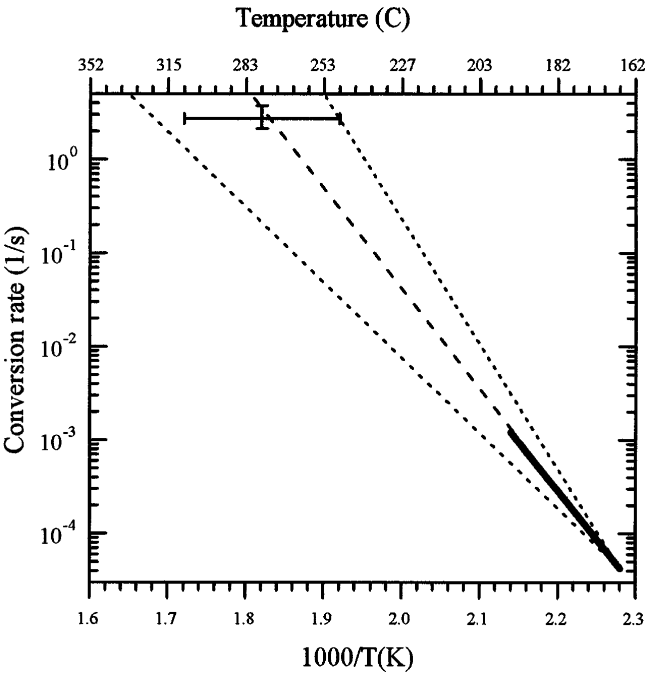

FIG. 3. Arrhenius plot of the rate constant as a function of temperature for the β-δ phase transition. The solid line is taken from an average of measurements by Brill *et al.* [6]. The dashed lines are an extrapolation of these data to high temperature, incorporating the quoted uncertainty. The data point at high temperature is from the laser ignition experiment reported here and is the inverse time to transition as a function of the inverse temperature.

two additional materials, CL-20 (2,4,6,8,10,12-hexanitro-2,4,5,8,10,12-hexaazatetracyclo $[5.5.0.0^{5,9}0.^{3,11}]$ dodecane) and TATB (1,3,5-triamino-2,4,6-trinitrobenzene) [19]. Measurements on these and other materials are ongoing in our laboratory.

We thank Darrin Naud and Mike Hiskey for preparation and characterization of β- and δ-HMX samples. We also acknowledge the support of the Laboratory Directed Research and Development Program of Los Alamos National Laboratory.

[1] J. Zinn and R. N. Rogers, J. Phys. Chem. **66**, 2646 (1962).

[2] G. Lengelle, A. Bizot, J. Duterque, and J.-C. Amiot, Rech. Aerosp. **2**, 1 (1991).

[3] B. W Asay, B. F. Henson, C. S. Fugard, and P. M. Dickson (to be published).

[4] *LASL Explosive Property Data*, edited by T. R. Gibbs and A. Popolato (University of California Press, Berkeley, 1980).

[5] H. H. Cady, A. C. Larson, and D. T. Cromer, Act. Crystallogr. Sect. B **16**, 617 (1963).

[6] T. B. Brill and R. J. Karpowicz, J. Phys. Chem. **86**, 4260 (1982).

[7] M. Herrmann, W. Engel, and N. Eisenreich, Propellants, Explos., Pyrotech. **17**, 190 (1992).

[8] T. B. Brill and C. O. Reese, J. Phys. Chem. **84**, 1376 (1980).

[9] F. Goetz, T. B. Brill, and J. R. Ferrarro, J. Phys. Chem. **82**, 1912 (1978); F. Goetz and T. B. Brill, J. Phys. Chem. **83**, 340 (1979).

[10] J. E. Davidson and M. W. Beckstead, Proceedings of the 26th International Symposium on Combustion (1996), p. 1989; K. Prasad, M. A. Tanoff, M. D. Smooke, and R. A. Yetter, in *Proceedings of the 33rd JANNAF Combustion Subcommittee Meeting* (Naval Postgraduate School, Monterey, CA, 1996), Vol. 2, p. 557.

[11] Y. R. Shen, *The Principles of Nonlinear Optics* (Wiley-Interscience, Toronto, 1984).

[12] B. F. Henson, K. R. Wilson, and J. M. Robinson, Phys. Rev. Lett. **79**, 1531 (1997); I. G. Voigt-Martin *et al.*, J. Phys. Chem. A **101**, 7265 (1997).

[13] The two polymorphs were synthesized from standard procedures and were identified by optical microscopy, FTIR, and index of refraction measurements on the ungraded powders.

[14] C. S. Choi and H. P. Boutin, Acta Crystallogr. Sect. B **26**, 1235 (1970).

[15] The complete mechanism will certainly include a reversible equilibrium (see, e.g., Ref. [6]).

[16] Changing crystal morphology or any higher order effects associated with the SHG dependence on the crystal morphology has not been addressed in this preliminary model.

[17] R. J. Karpowicz, L. S. Gelfand, and T. B. Brill, AIAA J. **21**, 310 (1983).

[18] F. P. Bowden and A. P. Yoffe, *Initiation and Growth of Explosions in Liquids and Solids* (Cambridge University Press, Cambridge, England, 1952).

[19] S. F. Son *et al.* (to be published).